
Article:
Ni, Feifan, Niu, Shuangxia, Li, Zhenghao et al. (1 more author) (2023) Novel Slot-opening PM Vernier Reluctance Machine with High-Order-Harmonic Winding. IEEE Transactions on Magnetics. ISSN 1941-0069

https://doi.org/10.1109/TMAG.2023.3296816

Novel Slot-opening-PM Vernier Reluctance Machine with High-Order-Harmonic Winding

Feifan Ni[1], Shuangxia Niu [1], *Senior Member IEEE* , Zhenghao Li[1] and Xing Zhao[2]

[1]Department of Electrical Engineering, The Hong Kong Polytechnic University, Hong Kong, 999077
[2]School of Physics, Engineering and Technology, The University of York, York YO10 5DD, UK

To combine the advantages of permanent magnet motor and electric excitation, a hybrid excitation Vernier reluctance motor is proposed in this paper. To make improved usage of working harmonics and relieve saturation effect in the stator core, a short-pitch distributed winding connection utilizing working harmonics modulated from fifth-order harmonics of DC excitation is newly applied to this machine, and tangentially-magnetized PMs are also introduced in this paper. The finite element analysis (FEA) simulation results verify that the proposed winding arrangement can achieve 26% higher output torque density compared to the conventional concentrated winding distribution and the slot PM can effectively alleviates the magnetic circuit saturation in the stator core.

***Index Terms*—Flux modulation, High-order-harmonic winding, Slot-opening PM, Vernier reluctance machine.**

I. Introduction

Permanent magnet motors have a wide range of application due to its high torque density and high efficiency [1]. However, rare-earth permanent magnet prices are rising, and researchers are focusing on reduced or nonrare-earth permanent magnet motors, such as the doubly fed doubly salient machine (DFDSM) and the variable flux reluctance machine (VFRM).

The DFDSM, where the PMs in the machine are replaced by the dc field windings has the disadvantage of high torque ripple because of its asymmetric magnetic circuit and resulted non-sinusoidal back-EMF [2]-[3]. In general, the VFRM with electrically dc-excited field has a robust rotor structure and is easy to manufacture [4]. VFRMs, however, distinctly reduce the torque ripple of the machine by optimizing the layout of the dc field winding to obtain a more symmetric magnetic circuit. However, the torque densities for both of the motors are still low because of the limited excitation capability of dc winding.

To solve this problem, Vernier reluctance machine (VRM) is proposed by some researchers, and flux modulation theory is introduced into the VFRMs to produce larger torque density. However, most of these Vernier motors apply full-pictched field windings [5]-[9]. This makes the motor prone to saturation and has poor overload performance.

In this paper, the field winding is arranged across three stator teeth. It has comparable torque density compared to conventional VRMs using full DC coils but reduces the DC copper losses and generates more richer harmonics in the airgap. Also, permanent magnets are inserted into the stator slots. This allows the paths of the flux generated by the permanent magnets to be parallel with that of the DC excitation, to achieve better flux regulation and alleviate the saturation in the stator core. To further improve the torque density and make full use of the higher -order working harmonics in the air gap, this paper proposes a new armature winding configuration that utilizes the higher-order harmonics of MMF generated by the DC winding.

The rest of the paper is organized as follows. In Section II, the machine structure, and the principle of the novel VRM with slot-opening PM is introduced and the parameters design is given. In Section III, fifth-order-harmonics winding designs are illustrated in detail and initial FEA validation is done. In Section IV, the electromagnetic performance of the traditional motor and novel motor are compared. Finally, the conclusions are drawn in Section V.

II. Slot-opening-PM Vernier Reluctance Machine

A. Machine structure

In this paper, a novel Vernier reluctance machine with slot-opening-PM which applied with fifth-order-harmonic winding design has been proposed, whose electromagnetic structure is shown in Fig.1. As shown in Fig.1, 18-slot and 13-pole-pair doubly salient structure is employed in this machine.

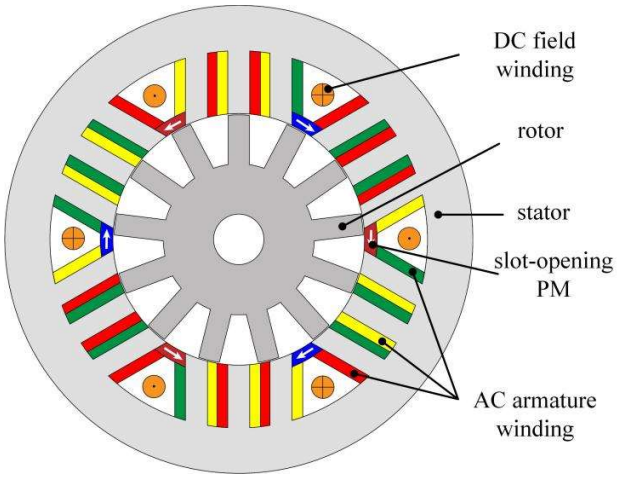

Fig. 1. Machine structure of 18/13 VRM with slot-opening PM

It has 18 stator slots housing two group of windings, which are DC field winding and armature winding respectively.

The DC field coils are wound across three stator teeth which has slot-opening PM. The AC winding adopted double layers distributed winding configuration. Due to the variable reluctance machine's doubly salient structure and unique DC winding configuration, there are many high order harmonics in

the airgap, and these harmonics can be further fully utilized to achieve an increase in output torque.

Because the conventional structure of an electrically excited doubly salient motor tends to saturate the stator core due to the bias field of the DC current, which limits the torque capability, especially under heavy-load condition.

B. Reliving-DC-Saturation Principle

The novel VRM is designed with slot-opening permanent magnets, whose magnetization direction is opposite with that of the DC excitation current. To better demonstrate the advantages of the slot-opening permanent magnet design, the flux path of the motor is provided in Fig.2.

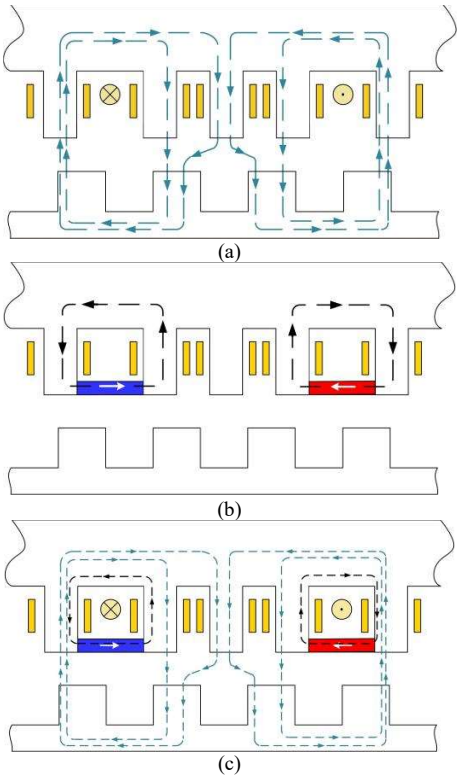

Fig. 2. The basic flax path of VRM (a) No PM, I_{dc}>0A (b) I_{dc}=0A (c) I_{dc}>0A

The magnetic circuit when there is only the DC current in the motor is shown in the Fig.2(a), and when there is a slotted permanent magnet acting, the resulting magnetic circuit is shown in the Fig.2(b). As can be seen from the Fig.2(c), when DC excitation and PM work simultaneously, it can relieve the saturation of the stator core, which means a higher DC current can be applied.

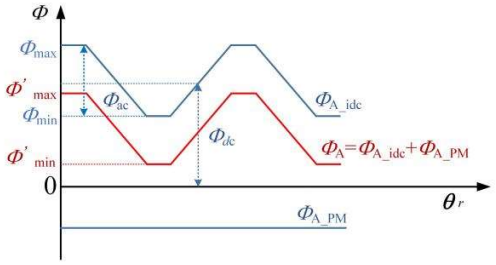

Fig. 3. Schematic of coil flux.

Specifically, due to the presence of the DC field winding, the coil flux has a DC bias. When no slot-opening PMs are present, the coil flux is shown in the Fig.3 as ϕ_{A_idc}, and the flux easily reaches saturation due to the presence of the DC bias ϕ_{dc}, which has no contribution to the back EMF. When the motor has slot-opening PMs, the flux produced by the permanent magnets is shown as ϕ_{A_PM}, and the total coil flux is shown as ϕ_A, which equals to $\phi_{A\_idc}+\phi_{A\_PM}$. With slot-opening PMs, the effect of DC bias is partially offset and the motor overload performance is improved.

C. Parameters design

The main parameters for the VRM machine are shown in the Table I. The other key geometry parameters for the VRM machine are shown in Fig.4.

TABLE I
MAIN PARAMETERS OF THE VRM WITH SLOT-OPENING PM

Parameters	Notation	Value
Number of stator slots	N_s	18
Number of rotor slots	N_r	13
Armature winding coil turns	n_{ac}	100
Field winding coil turns	n_{dc}	100
Armature current(A)	I_{ac}	5.67
Field current (A)	I_{dc}	8.5
Rotation speed (rpm)	v_r	60

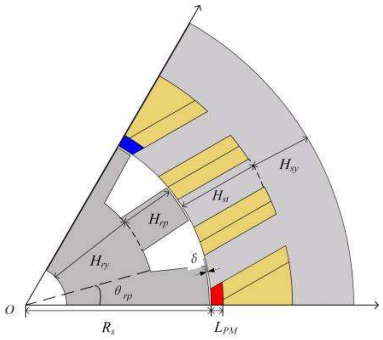

Fig. 4. Illustration of the geometric parameters of the proposed 18/13 VRM

All machines are globally optimized under the following fixed constraints.

1) Number of phases m = 3.
2) Stator outer radius R_{so}= 96 mm.
3) Shaft radius R_{shaft} = 12 mm.

Genetic algorithm (GA) is used to optimize the average torque while minimize torque ripple and the initial parameters are given in the Table II.

TABLE II
KEY GEOMETRY PARAMETERS OF THE VRM

Parameters	Notation	Value
Number of stator slots	N_s	18
Number of rotor slots	N_r	13
Stator's inner radius (mm)	R_s	54.2
Stator tooth height (mm)	H_{st}	20.3
Stator yoke height (mm)	H_{sy}	18
PM thickness (mm)	L_{PM}	3.61
Air gap length (mm)	δ	0.52
Rotor pole height (mm)	H_{rp}	15.94
Rotor yoke height (mm)	H_{ry}	25.98
Rotor pole width (deg)	θ_{rp}	29.5
Rotation speed (rpm)	v_r	60

III. Fifth-Order-Harmonics Winding Designs

A. Selection of the Main Working Harmonics

To further explain the merit of proposed winding design, the operating principle of the motor was analyzed as follows. Since the DC field coils are wound across three stator teeth, the fundamental pole pair number (PPN) of DC excitation, is calculated as (1),

$$N_p = \frac{N_s}{6} \tag{1}$$

where N_s is the number of stator slots. Based on the flux modulation theory, multiplying the expression for DC field winding's MMF with the expression for rotor permeance yields the air gap flux density,

$$B_r(\theta,t) = F_{DC}(\theta)P_r(\theta,t)$$
$$= \sum_{n=1}^{+\infty}\sum_{k=-\infty}^{+\infty}\frac{F_n P_{|k|}}{2}\sin\left(nN_p\theta + kN_r\theta - kN_r\omega t\right) \tag{2}$$

The working harmonics of winding configuration are modulated from dc field harmonic, whose PPNs can be expressed as follows:

$$P = \left|kN_p \pm N_r\right| \tag{3}$$

where N_r is the number of salient rotor poles. When $k = 1$,it means that the working harmonics are modulated from fundamental dc field harmonic. When $k > 1$ it means that the working harmonics are modulated from high-order dc field harmonic, which featured higher gear ratios. It is found that modulated by stator teeth, there is abundant of fifth-order harmonic in the air-gap flux density [10]. In this paper, working harmonics of the novel winding configuration are modulated from the fifth-order dc field harmonic, which means k is selected as 5.

According to modulation theory, the rotor angular velocity ω_m, the mechanical velocities of the working harmonics ω_{mec}, and the angular velocity of stator armature magnetic field have the following relationships.

$$G_r = \frac{\omega_{mec}}{\omega_m} = \frac{N_r}{P} \tag{4}$$

G_r is the gear ratio of the harmonics. In a magnetic field modulated motor, although the amplitude of the flux density of the air-gap working harmonic field is lower than that of the fundamental flux density, its rotational speed is G_r times the rotational speed of the fundamental flux density, so a larger back EMF can be induced, and the back EMF is calculated as follows.

$$E_{phn} = \frac{4.44DLT_{ph}}{60}(B_n k_{\omega n} G_r \omega_m) \tag{5}$$

where D is the diameter of the air-gap circumference, L is the stack length, T_{ph} is the number of turns in a phase, E_{phn} is the amplitude of back EMF contributed by nth harmonic, B_n is the amplitude of nth harmonic, $k_{\omega n}$ is the winding factor of n-th harmonic.

At the same time, since the fundamental magnetic field and the working harmonic magnetic field in the stator have the same electrical angular frequency, so they can act together to produce torque.

B. Winding configuration

According to Fig.1, the mechanical degree θ_m between two adjacent coils is related to the number of stator poles N_s, and it can be calculated by the following equation,

$$\theta_m = \frac{360}{N_s} \tag{6}$$

The number of electrical degrees θ between two adjacent teeth can be calculated as follows,

$$\theta = P\theta_m \tag{7}$$

The parameters of armature winding using proposed winding and conventional winding are given in Table III.

TABLE III
Parameters of Armature Winding Using Different Designs

Parameters	Proposed winding	Conventional winding
N_s, number of stator slots	18	18
θ_m, mechanical degree	20 deg	20 deg
P, pole pair number	2	10
θ, electrical degree	40 deg	200 deg
Coil pitch	4 slots	1 slot
Pole pitch	4.5 slots	0.9 slot
Pitch factor	0.9848	0.988
Distribution factor	0.9598	0.844
Winding factor	0.9452	0.834

By choosing the high-order harmonic as the working harmonic, a higher distribution factor and winding factor can be achieved. The novel winding design can not only utilize the fundamental dc field harmonic, but also the high-order harmonic whose pole pair number is small to produce the back EMF. In order to achieve a higher gear ratio, the smaller the pole pair number of the high-order harmonic winding design the better. Thus, the fifth-order harmonic is chosen for the proposed design in this paper.

Fig.5 depicts the detailed back EMF phasors of each slot in both designs. The EMF phases n and n' on the backside of the coil have opposite polarities. It can be noted that that in 18/13-pole doubly salient machines, the reverse connection of the coil occurs when the two phases have a phase shift of 180 degrees.

The conventional winding is more suitable for concentrated windings, whose coil pitch is one slot. In comparison, higher winding factor can be achieved, when short-pitched double-layers distributed winding configuration whose coil pitch is 4 slots is applied.

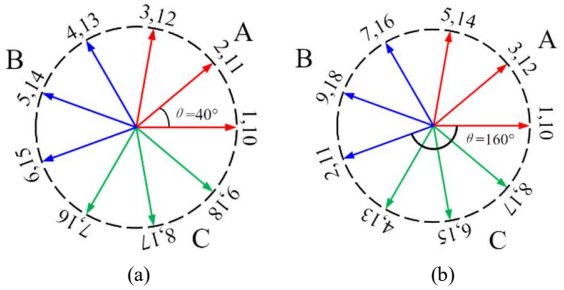

(a) (b)

Fig. 5. Coil back EMF phasors. (a) Proposed winding. (b) Conventional winding.

C. Initial FEA Validation of Air-gap harmonics

The calculated air-gap harmonics distribution of this hybrid excitation 18/13 VRM is presented in Fig.6. In two different

winding configurations, the main operating harmonics used are further highlighted in red and blue.

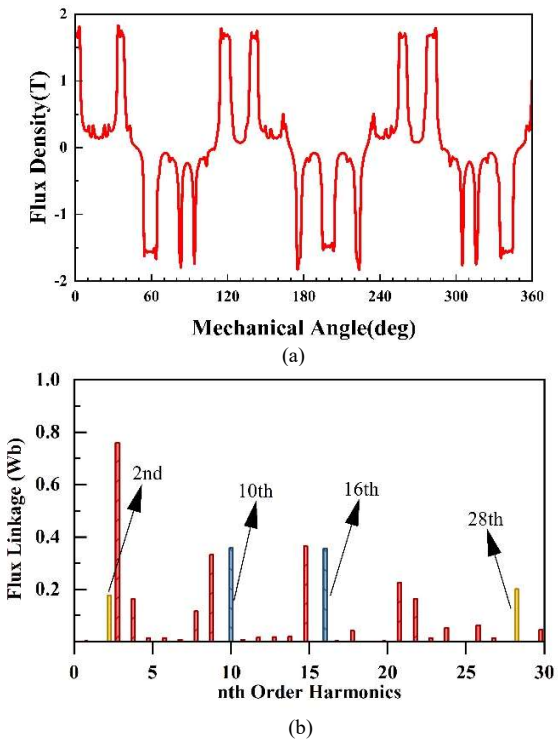

Fig. 6. air-gap flux density. (a) Waveform. (b) Harmonics.

It can be seen from the results that there is component modulated from the fundamental dc field harmonic, whose PPN is $|N_p \pm N_r|$,which are 10 and 16 in this model. When the dc field windings and PMs are distributed every three stator teeth, higher order harmonics are generated in the motor air gap, such as the fifth harmonic, whose PPN equals to $|5N_p \pm N_r|$, which are 2 and 28 in this model.

Although the fifth harmonics whose PPN is 2 has the amplitude of 0.18Wb, the gear ratio of this harmonic is 6.5. The amplitude of the fundamental harmonic is 0.38Wb, but the gear ratio is only 1.3. From the analyze above, the conclusion can be drawn that the fifth-order harmonic's rotational speed is much larger than fundamental harmonic. Thus, the proposed armature winding design, that utilize the harmonic whose PPN is 2, can produced higher back EMF and larger output torque than conventional design that utilize the harmonic whose PPN is 10.

IV. Performance Comparison

To demonstrate the characteristics of the proposed new motor, the conventional motor is also presented for comparison. The finite element method is used to analyze these motors. Fig.7 shows the configurations of these motors. As shown in Fig. 7, the Model I is the proposed motor with slot-opening-PM and proposed novel winding configuration modulated from fifth-order dc field harmonic. The Model II has the same mechanical structure as the Model I, but with a conventional centralized winding. The Model III is the conventional motor without slot-opening-PM but apply the proposed high-order winding design. The Model IV has no slot-opening-PM with traditional winding design.

A. Flux density

The magnetic flux density of the models is shown in Fig.7.

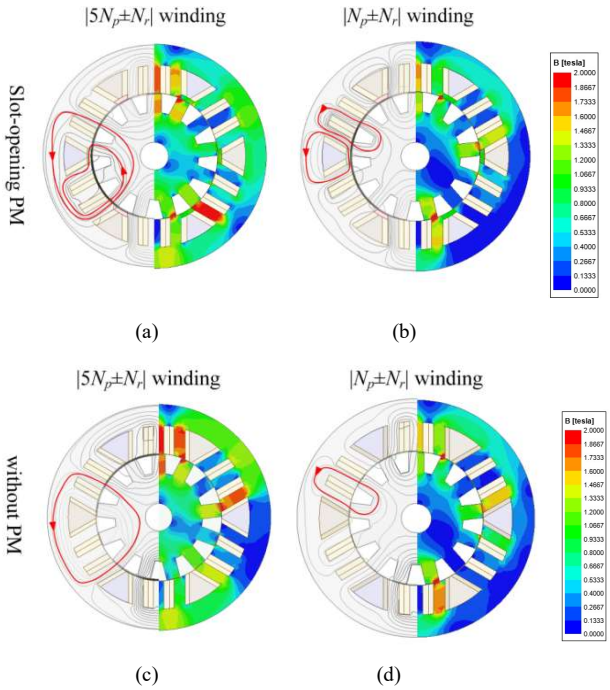

Fig. 7. Comparison of flux path and distribution I_{dc}=0A, I_{ac}>0A. (a) Model I. (b) Model II.(c) Model III. (d) Model IV.

Since the distribution of the dc field windings is the same for all four models, they produce the same magnetic field distribution. However, due to the difference in the distribution of the slot-opening permanent magnets and the ac winding, the magnetic field distribution of these four models is different.

By comparing the model with conventional winding (Model II and Model IV) and the model with the proposed novel winding (Model I and Model III), it can be found that the model with the novel winding has a longer flux path due to its lower pole pair number than the model with the conventional winding.

Comparing the results of the model with slot-opening permanent magnets (Model I and Model II) and the model without slotted permanent magnets (Model III and Model IV), it can be found that slotted permanent magnets can reduce saturation, which is consistent with the previous theory.

B. Back EMF

The back EMF waveforms for the four models are shown in the Fig.8, and the specific results are listed in the Table IV.

TABLE IV
COMPARISON OF PHASE BACK EMF

Model	Slot-opening PM	Winding	Amplitude of Back EMF
Model I	Slot-opening PM	proposed	21 V
Model II	Slot-opening PM	conventional	13 V
Model III	Without slot-opening PM	proposed	21 V
Model IV	Without slot-opening PM	conventional	13 V

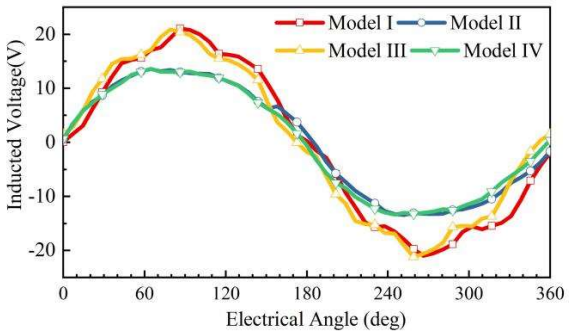

Fig. 8. Comparison of phase back EMF.

The result shows that the amplitude of the back EMF Model I is about 62% higher than that of Model II, and the amplitude of Model III is about 60% higher than that of Model IV. This means that the apply of the proposed winding design can increase the back EMF of the motor, which is consistent with the modulation theory.

By comparing the models with slot-opening PM (Models I and II) and the models without PM (Models III and IV), it can be found that the use of slot-opening PM can not increase the back EMF of the motor, which is consistent with the above theoretical derivation.

C. Electromagnetic torque

When the motor is at rated current excitation, the torque of four models are shown in the Fig.9.

The torque ripple is defined as below,

$$R_T = \frac{T_{max} - T_{min}}{T_{avg}} \tag{8}$$

where T_{max} is the maximum of the torque, T_{min} is the minimum of the torque, T_{avg} is the average torque. The specific torque production results are compared in the Table IV.

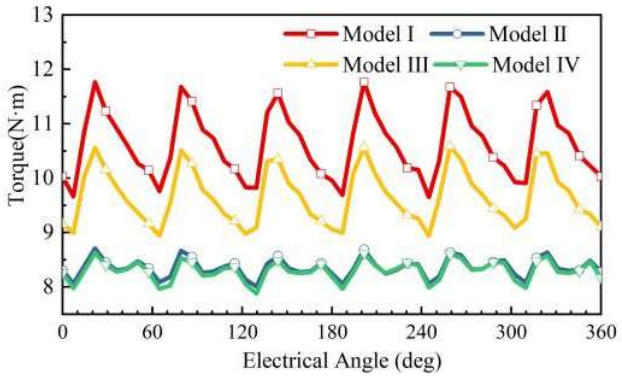

Fig. 9. Comparison of torque production.

TABLE IV
COMPARISON OF TORQUE PRODUCTION

Model	I	II	III	IV
T_{avg}, Average torque (N·m)	10.6	8.4	9.6	8.3
T_{max}, Maximum of torque (N·m)	11.7	8.7	10.6	8.6
T_{min}, Minimum of torque (N·m)	9.6	8.0	8.9	7.8
T_d, Torque density (kN·m/mm^3)	5.3	4.2	4.8	4.2
T_{pm}, Unit PM output (kN·m/mm^3)	736	583	-	-
R_T, Torque ripple	19%	8%	17%	8%

Due to the high back-EMF, Model I exhibits 26% higher torque than Model II and Model III exhibits 16% higher than Model IV. This shows that the proposed armature winding design can improve the torque density than conventional winding design due to the utilization of fifth-order space harmonics in magnetic field.

Define the torque density and the unit permanent magnet output as below,

$$T_d = \frac{T_{avg}}{V} \tag{9}$$

$$T_{pm} = \frac{T_{avg}}{V_{pm}} \tag{10}$$

The torque density of Model I is 5.3kNm/mm^3. It is lower compared to traditional permanent magnet motor whose torque density is about 10kNm/mm^3, but the unit permanent magnet output can achieve 736kNm/mm^3.

D. Electromagnetic torque

The power factor and efficiency of these four models are also compared in the Fig.10.

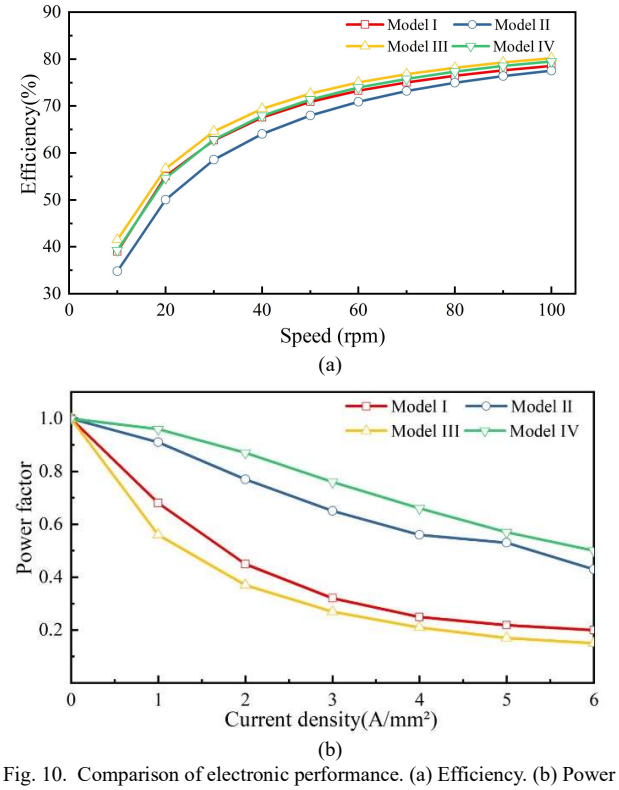

Fig. 10. Comparison of electronic performance. (a) Efficiency. (b) Power factor.

It is admitted that the model in this paper with proposed winding design has lower power factor and higher copper loss than traditional winding design unless a larger ratio of length and diameter is applied.

E. Overload capacity

To further study the influence of slot-opening permanent magnets on the overload capacity of the motor, Model I and Model III are further analyzed.

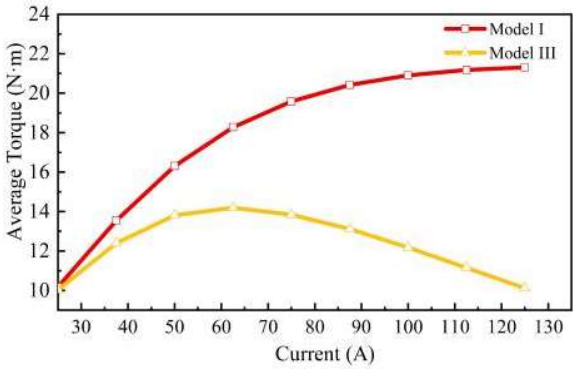

Fig. 11. Comparison of torque under different load.

The VRM with slot-opening PM (Model I) and the VRM without slot-opening PM (Model III) are compared under different armature current. When the current density is rated, Model I exhibits a little higher torque than Model III. The torque of Model III begin to drop when the current is about 2.5 times of the rated-current. However, Model I still exhibits high torque when the current is 5 times of the rated-current as is shown in the Fig.11.

The result shows that the motor with slot-opening PM has higher torque production under the same winding design, especially at high-load current density.

V. Conclusion

In this paper, a 18s/13r relieving-DC-saturation slot-opening-PM hybrid Vernier reluctance machine with newly winding connection utilizing working harmonics modulated from fifth-order harmonics in the air gap is proposed for higher output torque capability. Meanwhile, slot-opening PMs can further reduce the saturation of the stator core of the motor and thus improve the overload capacity of the motor.

According to the FEA results, the torque output is increased by 26% under load compared to the motor with the conventional winding arrangement, with a small increase in torque fluctuation compared to the conventional winding motor, which can be further suppressed by the subsequent optimized control algorithm. At rated load, the motor with slot PMs could achieve 10% higher output torque than that of the motor without slot-opening permanent magnets. Simulation results also show that the motor with slot-opening PMs has better performance under heavy load condition. The benefits of the proposed motor structure are high torque density, and hybrid excitation for easy magnetization. Therefore, it is suitable for applications with wide speed range, such as electric vehicle motors.

Acknowledgement

This work was supported by the Research Grant Council of the Hong Kong Government under Project PolyU 152109/20E.

References

[1] S. Zheng, X. Zhu, L. Xu, T. Zhu and D. Wu, "Comparative Analysis and Multi-Objective Optimization of Hybrid Permanent Magnet Motors Considering Different Saliency Characteristics," in IEEE Transactions on Applied Superconductivity, vol. 31, no. 8, pp. 1-5, Nov. 2021, Art no. 5205205, doi: 10.1109/TASC.2021.3091066.

[2] Y. Fan, K. T. Chau and S. Niu, "Development of a New Brushless Doubly Fed Doubly Salient Machine for Wind Power Generation," in IEEE Transactions on Magnetics, vol. 42, no. 10, pp. 3455-3457, Oct. 2006, doi: 10.1109/TMAG.2006.879435.

[3] Y. Fan and K. T. Chau, "Design, Modeling, and Analysis of a Brushless Doubly Fed Doubly Salient Machine for Electric Vehicles," in IEEE Transactions on Industry Applications, vol. 44, no. 3, pp. 727-734, May-june 2008, doi: 10.1109/TIA.2008.921406.

[4] X. Liu and Z. Q. Zhu, "Comparative Study of Novel Variable Flux Reluctance Machines With Doubly Fed Doubly Salient Machines," in IEEE Transactions on Magnetics, vol. 49, no. 7, pp. 3838-3841, July 2013, doi: 10.1109/TMAG.2013.2242047.

[5] S. Jia, R. Qu and J. Li, "Analysis of the Power Factor of Stator DC-Excited Vernier Reluctance Machines," in IEEE Transactions on Magnetics, vol. 51, no. 11, pp. 1-4, Nov. 2015, Art no. 8207704, doi: 10.1109/TMAG.2015.2450493.

[6] S. Jia, K. Yan, D. Liang and J. Liu, "Research on the Reactive Power Regulation Capability of Stator DC Current Excited Vernier Reluctance Machine," 2019 22nd International Conference on Electrical Machines and Systems (ICEMS), Harbin, China, 2019, pp. 1-5, doi: 10.1109/ICEMS.2019.8921936.

[7] D. Thyroff and I. Hahn, "Investigation of an Electrically Excited Vernier Machine with a Concentrated Winding intended for Traction Applications," 2019 26th International Workshop on Electric Drives: Improvement in Efficiency of Electric Drives (IWED), Moscow, Russia, 2019, pp. 1-5, doi: 10.1109/IWED.2019.8664396.

[8] L. Huang, Z. Q. Zhu, J. Feng, S. Guo and J. X. Shi, "Comparative Analysis of Variable Flux Reluctance Machines With Double- and Single-Layer Concentrated Armature Windings," in IEEE Transactions on Industry Applications, vol. 55, no. 2, pp. 1505-1515, March-April 2019, doi: 10.1109/TIA.2018.2884608.

[9] W. Wang, X. Zhao, S. Niu and W. Fu, "Comparative Analysis and Optimization of Novel Pulse Injection Sensorless Drive Methods for Fault-Tolerant DC Vernier Reluctance Machine," in IEEE Transactions on Power Electronics, vol. 37, no. 11, pp. 13566-13576, Nov. 2022, doi: 10.1109/TPEL.2022.3182054.

[10] X. Zhao, S. Wang, S. Niu, W. Fu and X. Zhang, "A Novel High-Order-Harmonic Winding Design Method for Vernier Reluctance Machine With DC Coils Across Two Stator Teeth," in *IEEE Transactions on Industrial Electronics*, vol. 69, no. 8, pp. 7696-7707, Au